RESEARCH ARTICLE

Claudin-15 overexpression inhibits proliferation and promotes apoptosis of Schwann cells *in vitro*

Jian-Nan Li[1], Zhan Zhang[1], Guang-Zhi Wu[1], Deng-Bing Yao[2], Shu-Sen Cui[1,*]
1 China-Japan Union Hospital of Jilin University, Changchun, Jilin Province, China
2 School of Life Sciences, Jiangsu Key Laboratory of Neuroregeneration, Co-innovation Center of Neuroregeneration, Nantong University, Nantong, Jiangsu Province, China

Funding: *This study was supported by the National Natural Science Foundation of China, No. 81671220 (to SSC); the Scientific and Technological Development Program of Jilin Province of China, No. 20160101077JC (to SSC); the School Joint Construction Special Project of Jilin Province of China, No. SXGJQY2017-13 (to SSC).*

Graphical Abstract

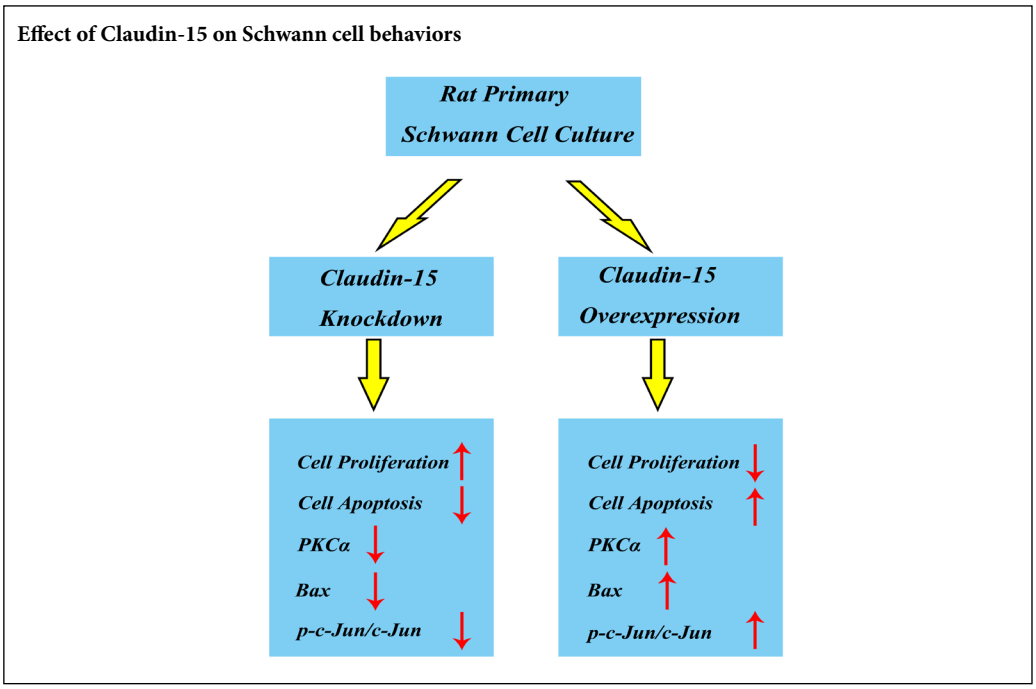

Correspondence to:
Shu-Sen Cui, PhD, MD, sscui916@126.com.

orcid:
0000-0003-2840-8166 (Shu-Sen Cui)

doi: *10.4103/1673-5374.264463*

Received: *November 24, 2018*
Accepted: *March 28, 2019*

Abstract

Our previous experiments have discovered that Claudin-15 was up-regulated in Schwann cells of the distal nerve stumps of rat models of sciatic nerve injury. However, how Claudin-15 affects Schwann cell function is still unknown. This study aimed to identify the effects of Claudin-15 on proliferation and apoptosis of Schwann cells cultured *in vitro* and explore the underlying mechanisms. Primary Schwann cells were obtained from rats. Claudin-15 in Schwann cells was knocked down using siRNA (siRNA-1 group) compared with the negative control siRNA transfection group (negative control group). Claudin-15 in Schwann cells was overexpressed using pGV230-Claudin-15 plasmid (pGV230-Claudin-15 group). The pGV230 transfection group (pGV230 group) acted as the control of the pGV230-Claudin-15 group. Cell proliferation was analyzed with EdU assay. Cell apoptosis was analyzed with flow cytometric analysis. Cell migration was analyzed with Transwell inserts. The mRNA and protein expressions were analyzed with quantitative polymerase chain reaction assay and western blot assay. The results showed that compared with the negative control group, cell proliferation rate was up-regulated; p-AKT/AKT ratio, apoptotic rate, p-c-Jun/c-Jun ratio, mRNA expression of protein kinase C alpha, Bcl-2 and Bax were down-regulated; and mRNA expression of neurotrophins basic fibroblast growth factor and neurotrophin-3 were increased in the siRNA-1 group. No significant difference was found in cell migration between the negative control and siRNA-1 groups. Compared with the pGV230 group, the cell proliferation rate was down-regulated; apoptotic rate, p-c-Jun/c-Jun ratio and c-Fos protein expression increased; mRNA expression of protein kinase C alpha and Bax decreased; and mRNA expressions of neurotrophins basic fibroblast growth factor and neurotrophin-3 were up-regulated in the pGV230-Claudin-15 group. The above results demonstrated that overexpression of Claudin-15 inhibited Schwann cell proliferation and promoted Schwann cell apoptosis *in vitro*. Silencing of Claudin-15 had the reverse effect and provided neuroprotective effect. This study was approved by the Experimental Animal Ethics Committee of Jilin University of China (approval No. 2016-nsfc001) on March 5, 2016.

Key Words: *apoptosis; Bax; cell proliferation; c-Jun; Claudin-15; nerve regeneration; peripheral nerve injury; protein kinase C alpha; Schwann cells; Wallerian degeneration*

Chinese Library Classification No. *R453; R363; R364*

Introduction

Many patients present with peripheral nerve injury every year (Siemionow and Brzezicki, 2009). This commonly results in Wallerian degeneration (Conforti et al., 2014; Cao et al., 2019), first discovered by Waller (1851). The discovery of WLDS protein in strains of mice resistant to axonal degeneration (Mack et al., 2001; Coleman and Freeman, 2010; Williams et al., 2017) convinced researchers that Wallerian degeneration is a programmed cell event (Gerdts et al., 2016; Wang et al., 2018). In normal mice, immediately after peripheral nerves suffer trauma, Wallerian degeneration begins (Girouard et al., 2018); the disintegration of axonal structures occurs (Geden and Deshmukh, 2016; Simon et al., 2016), atrophy of fiber tracts is observed and macrophages and Schwann cells infiltrate (Liou et al., 2011; Simon et al., 2016; Zigmond and Echevarria, 2019).

In the peripheral nervous system, Schwann cells wrap around the nerve fibers and secrete neurotrophins to protect and nourish the peripheral nerves (Kennedy and Zochodne, 2005; Jortner, 2019). During Wallerian degeneration, Schwann cells play a vital role in the degeneration and regeneration of neurons (Jessen and Arthur-Farraj, 2019; Jessen and Mirsky, 2019; Shefa and Jung, 2019; Yi et al., 2019). The Schwann cells release a variety of factors associated with apoptosis (Li et al., 2018; Zhang et al., 2018) and participate in the clearance of myelin debris (Namikawa et al., 2006; Lindborg et al., 2017). Schwann cells proliferate (Liu et al., 2019), dedifferentiate and migrate, offering regenerating axons both the structural direction and the growth promotion factors (Tetzlaff, 1982; Stoll et al., 2002; Jessen and Mirsky, 2016). Nevertheless, how Schwann cells participate in Wallerian degeneration remains unclear.

Claudins are the main constituents of the tight junction membrane proteins. At least 27 Claudins have been discovered (Morita et al., 1999; Van Itallie and Anderson, 2006; Muto, 2017; Tsukita et al., 2019). Claudins are the key molecules that maintain cell polarity and molecular transport (Hagen, 2017). Commonly, Claudins form chains that mediate cell adhesion and function as barriers to cells (Krause et al., 2015; Tsukita et al., 2019). They have also been shown to function as ion channels and regulate homeostasis and inflammation (Garcia-Hernandez et al., 2017; Alberini et al., 2018).

Claudins are expressed in Schwann cells (Manole et al., 2015). Claudin family members Claudin-14 and Claudin-15 are classic tight junction molecules (Krause et al., 2008) that we discovered were expressing in Schwann cells of the sciatic nerve after peripheral nerve injury (Li et al., 2013; Gong et al., 2014). The molecular mechanism underlying how Claudin-15 affects Schwann cell functions was poorly understood. This study explores the functions of Claudin-15 on cell proliferation, apoptosis and migration in cultured Schwann cells.

Materials and Methods

Schwann cells culture and transfection

Schwann cells were cultured according to the protocols described previously (Li et al., 2013; Zhang et al., 2018). Primary Schwann cells were extracted and isolated from the sciatic nerves of one-day old Sprague-Dawley rats (Experimental Animal Center of Jilin University, China; license No. SCXK (Ji) 2002-0002). Primary Schwann cells were cultured in Dulbecco's modified Eagle's medium (Sigma, Saint Louis, MO, USA) containing 10% fetal bovine serum (Gibco, New York, USA) and penicillin-streptomycin solution (Beyotime, Jiangsu, China) at 37°C with 5% CO_2. Fibroblasts were destroyed by complement cleavage using polyclonal anti-Thy1.1 antiserum (Sigma). Recombinant human NRG1-beta 1/HRG1-beta 1 epidermal growth factor Domain Protein (R&D system, Minneapolis, MN, USA) and forskolin (Sigma) were added to the media for cell proliferation.

Schwann cells were transfected separately with siRNA-1, siRNA-2 and siRNA-3 (RiboBio, Guangzhou, China; Table 1) using Lipofectamine 3000 reagent (Invitrogen, New York, NJ, USA) for Claudin-15 knockdown (n = 3). A negative control siRNA transfection group (**Table 1**) was used as the control group for Claudin-15 knockdown. Schwann cells were transfected with pGV230-CLDN15 plasmid using Lipofectamine 3000 reagent for overexpression of Claudin-15 (n = 3). Transfection with pGV230 acted as the control group. RNA was collected 48 hours after transfection. Proteins were collected and assessed 72 hours after transfection. Schwann cells were planted on the Transwell insert 48 hours after transfection. Cell proliferation assay and cell apoptosis assay were done 72 hours after transfection. Every experimental procedure and protocol was approved by the Experimental Animal Ethics Committee of Jilin University of China (approval No. 2016-nsfc001) on March 5, 2016.

RNA isolation and real-time quantitative polymerase chain reaction (PCR) assay

Total RNA was isolated from Schwann cells following the manufacturer's protocols. Real-time quantitative PCR was accomplished with TB Green™ Fast qPCR Mix (Takara, Kusatsu, Japan). Primer sequences of Bax: Bcl-2-Associated X

Table 1 Claudin-15 siRNA primers

Gene	Sequence	Product size (bp)
NC	Forward: 5′ UUC UCC GAA CGU GUC ACG UTT 3′	21
	Reverse: 5′ ACG UGA CAC GUU CGG AGA ATT 3′	21
siRNA-1	Forward: 5′ GGA ACG UCA UCA CCC ACU AAC A 3′	22
	Reverse: 5′ UUA GAG GUG AGG ACG UUC CCA 3′	22
siRNA-2	Forward: 5′ GGA GAG UGU CUA CCG UCC AUG 3′	21
	Reverse: 5′ UGG ACG GUA GAC ACU CUC CAG 3′	21
siRNA-3	Forward: 5′ GGG UGG GAC UUC CCU ACA AGC 3′	21
	Reverse: 5′ UUG UAG GGA AGU CCC ACC CUG 3′	21

siRNA: Small interfering RNA; NC: negative control.

protein (Bax, pro-apoptosis factor), B-cell lymphoma 2 (Bcl-2, anti-apoptosis factor), basic fibroblast growth factor (bFGF, neurotrophin), neurofibromin 2 (Nf2, cytoskeleton-associated protein), neurotrophin-3 (NT3), protein kinase C alpha (PKCα, serine threonine kinase) are listed in **Table 2**. Relative mRNA expression levels were calculated using the relative quantitation comparative CT method ($2^{-\Delta\Delta Ct}$ method) (Li et al., 2018; Zhang et al., 2018). Each sample was run in triplicate.

Cell proliferation assay

The assay of cell proliferation was performed with Cell-Light Apollo567 *In Vitro* Kit (RiboBio, Guangzhou, China). Complete medium was used to re-suspend the Schwann cells that were then tallied and plated on 96-well poly-L-lysine-coated plates. EdU was applied and the cells were cultured after cell transfection. The cells were fixed with phosphate buffered saline containing 4% formaldehyde and stained with Apollo 567 (RiboBio, Guangzhou, China) and Hoechst 33342 (RiboBio). Schwann cell proliferation analysis was performed using randomly selected images through a fluorescence microscope (Leica, Mannheim, Germany). The proliferating cell numbers were calculated. The average number of proliferating cells in the control group was set as 100%. The cell proliferation rate of p-GV230-Claudin-15 group was obtained by dividing by the average number of proliferating cells in the negative control or pGV230 group. The results were presented as fold change.

Table 2 Primers used in real-time quantitative polymerase chain reaction

Name	Sequence	Product size (bp)
CLDN15	Forward: 5′-CGG GCA GAA GCA ATC AGA C-3′	93
	Reverse: 5′-AAG ACT GAG GAG GGA GAA GGT T-3′	
Bax	Forward: 5′-TGC AGA GGA TGA TTG CTG AC-3′	173
	Reverse: 5′-GAT CAG CTC GGG CAC TTT AG-3′	
Bcl-2	Forward: 5′-GCA GAG ATG TCC AGT CAG C-3′	129
	Reverse: 5′-CCC ACC GAA CTC AAA GAA GG-3′	
bFGF	Forward: 5′-CCC GCA CCC TAT CCC TTC ACA GC-3′	130
	Reverse: 5′-CAC AAC GAC CAG CCT TCC ACC CAA A-3′	
Nf2	Forward: 5′-CTG GGA TTG GGT TCA TGG GTG GAT-3′	127
	Reverse: 5′-AGG AAG CCC GAG AAG CAG AGC G-3′	
NT3	Forward: 5′-GAC AAG TCC TCA GCC ATT GAC ATT C-3′	131
	Reverse: 5′-CTG GCT TCT TTA CAC CTC GTT TCA T-3′	
PKCα	Forward: 5′-GAA CAC ATG ATG GAC GGG GTC ACG AC-3′	170
	Reverse: 5′-CGC TTG GCA GGG TGT TTG GTC ATA-3′	
GAPDH	Forward: 5′-GCA AGT TCA ACG GCA CAG-3′	141
	Reverse: 5′-CGC CAG TAG ACT CCA CGA C-3′	

Bax: Bcl-2-associated X protein; Bcl-2: B-cell lymphoma 2; bFGF: basic fibroblast growth factor; CLDN15: claudin 15; GAPDH: glyceraldehyde-3-phosphate dehydrogenase; Nf2: neurofibromin 2; NT3: neurotrophin-3; PKCα: protein kinase C alpha.

Flow cytometric analysis

Cell apoptosis was probed using Annexin V-FITC Apoptosis Detection Kit (Beyotime, Jiangsu, China). The Schwann cells were trypsinized, ultra-centrifuged, and resuspended. Annexin V-FITC solution was dropped onto each sample and left to stand for 15 minutes. Cells were resuspended. Propidium iodide reagent was dropped onto the samples, which were then kept in the dark for 15 minutes at room temperature. The cells were analyzed by Beckman Flow Cytometer (Beckman, Fullerton, CA, USA). The average rate of apoptosis in the control group was set as 100%. The cell apoptotic rate of p-GV230-Claudin-15 group was obtained by dividing it with the average rate in the negative control or pGV230 group. The results were exhibited as fold change.

Cell migration assay

Cell migration was assayed using Transwell inserts (Corning Inc, Corning, NY, USA) (Mantuano et al., 2008). The membrane of each insert was coated with fibronectin (Sigma). Schwann cells were planted in the top chamber with Dulbecco's modified Eagle's medium. The lower chambers contained complete medium. After 24 hours, the migrated Schwann cells were fixed with methanol and stained with crystal violet solution. The non-migrated cells in the upper chamber were wiped with cotton swabs. Migrated cells were imaged and tallied using a DMR inverted microscope (Leica, Mannheim, Germany). The migrated cell numbers were calculated, taking the average number of migrated cells in control group as 100%. The cell migration rate of the p-GV230-Claudin-15 group was obtained by dividing it with the average number of negative control or pGV230 group. The results were exhibited as fold changes.

Western blot assay

Schwann cells were prepared with RIPA lysis buffer (Sangon Biotech, Shanghai, China) and their protein concentrations were evaluated by BCA Protein Assay Kit (Beyotime, Jiangsu/Shanghai, China). The protein was electrophoresed through a 12% sodium dodecyl sulfate polyacrylamide gel and then transferred to polyvinylidene fluoride membranes. The membranes were blocked by 5% bovine serum albumin in Tris-buffered saline Tween-20 for 1 hour at room temperature. The membranes were incubated with primary antibodies at 4°C overnight: rabbit polyclonal anti-Claudin 15 antibody (1:200; Santa Cruz Biotechnology, Santa Cruz, CA, USA); rabbit monoclonal anti-AKT antibody (1:1000; CST, Boston, MA, USA) (AKT pathway pro-survival factor); rabbit monoclonal anti-phospho-AKT antibody (1:1000; CST)

(AKT pathway pro-survival factor); rabbit monoclonal anti-ERK1/2 antibody (1:1000; CST) (ERK pathway pro-survival factor); rabbit monoclonal anti-phospho-ERK1/2 (1:1000; CST) (ERK pathway pro-survival factor); mouse monoclonal anti-c-Jun antibody (1:200, Santa Cruz Biotechnology) (JNK pathway pro-apoptosis factor); mouse monoclonal anti-p-c-Jun antibody (1:200; Santa Cruz Biotechnology) (JNK pathway pro-apoptosis factor); rabbit monoclonal anti-β-Catenin antibody (1:5000; Abcam, Cambridge, MA, USA) (WNT pathway cell adhesion factor); rabbit polyclonal anti-c-Fos antibody (1:250; Abcam) (JNK pathway transcription factor); rabbit monoclonal anti-GAPDH antibody (1:10,000; Abcam). The next day, the membranes were incubated with secondary antibody, either horseradish peroxidase-labeled goat anti-mouse IgG (1:1000; Beyotime) or horseradish peroxidase-labeled goat anti-rabbit IgG, for 2 hours at room temperature. Protein expression levels were normalized with reference to GAPDH. Images were scanned by a GS800 Densitometer Scanner. The blot intensity was evaluated by Multi Gauge software (Fuji, Tokyo, Japan). The blot intensity was first normalized with respect to that of GAPDH in each group. The average blot density of control group was set as 100%. The relative optical density value of p-GV230-Claudin-15 group was obtained by dividing them with the optical density values of the negative control or pGV230 group.

Statistical analysis

All data are expressed as the mean ± SD, and analyzed using SPSS 15.0 software (SPSS, Chicago, USA). The data were analyzed with two tailed, unpaired Student's *t*-test and one-way analysis of variance followed by Tukey's *post hoc* test. $P < 0.05$ was considered statistically significant.

Results

siRNA and plasmid selection

Our previous research showed that the expression of Claudin-15 was up-regulated in Schwann cells of rat sciatic nerve after peripheral nerve injury (Li et al., 2013). The three specific Claudin-15 siRNAs listed in **Table 1** were synthesized by RiboBio. Claudin-15 expression in cultured Schwann cells was significantly decreased at the mRNA level by siRNA-1 transfection (**Figure 1**). The expression of Claudin-15 declined more than 80% with siRNA-1 (**Figure 1**). Hence, siRNA-1 was chosen for following experiments. We used the pGV230-Claudin-15 plasmid for Claudin-15 overexpression analysis (**Figure 1**).

Claudin-15 affects several gene expression changes of cultured Schwann cells

To further investigate the functions of Claudin-15 on expressions and relative factors release in Schwann cells, we analyzed Bcl-2, Bax, bFGF, PKCα, NT3 and Nf2 expressions. These factors are related to nerve degeneration and regeneration after Claudin-15 overexpression and knockdown in transfected Schwann cells. In Claudin-15 knockdown Schwann cells, the expressions of Bax, Bcl-2 and PKCα decreased, whereas bFGF and NT3 were up-regulated (**Figure 2A**). The expressions of Bax and PKCα increased, whilst NT3 and bFGF were down-regulated in Schwann cells with over expressed Claudin-15 (**Figure 2B**). These results suggest that differential expression of Claudin-15 resulted in expression changes of other factors in Schwann cells.

Claudin-15 inhibits Schwann cells proliferation *in vitro*

We analyzed the action of Claudin-15 on the proliferation of Schwann cells. After transfection with Claudin-15 siRNA-1, pGV230-Claudin-15 plasmid or negative control, EdU proliferation assay demonstrated that the proliferation proportion of cultured Schwann cells after siRNA transfection significantly increased compared with that of the negative control ($P < 0.05$; **Figure 3A**, **B,** and **E**). On the other hand, when Schwann cells were transfected with pGV230-Claudin-15

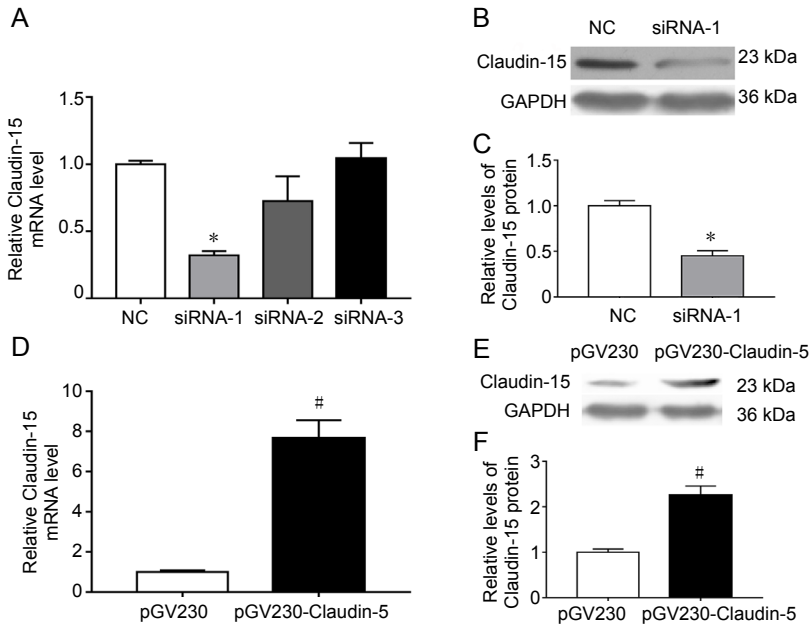

Figure 1 Claudin-15 mRNA expression changes after siRNA knockdown and overexpression in cultured Schwann cells.

(A) Relative levels of Claudin-15 mRNA expression after siRNA transfection compared to the negative control. (B) Western blot assay of Claudin-15 after siRNA transfection. The upper panel shows target bands of Claudin-15; the lower panel shows the loading control GAPDH. (C) Relative levels of Claudin-15 protein expression after siRNA transfection. (D) Relative levels of Claudin-15 mRNA expression after pGV230-Claudin-15 transfection. (E) Western blot assay of Claudin-15 after pGV230-Claudin-15 transfection. The upper panel shows target bands of Claudin-15; the lower panel shows the loading control GAPDH. (F) Relative levels of Claudin-15 protein expression after pGV230-Claudin-15 transfection. *$P < 0.05$, *vs.* NC group; #$P < 0.05$, *vs.* pGV230 group. Average blot density of control group blot was set as 100%. The relative optical density value of p-GV230-Claudin-15 group was obtained by dividing its optical density with the optical density values of the NC or pGV230 group. Assays were performed in triplicate. Data are shown as the mean ± SEM (A: Unpaired Student's *t*-test; C, D, F: one-way analysis of variance followed by Tukey's *post hoc* test). GAPDH: Gyceraldehyde-3-phosphate dehydrogenase; NC: negative control.

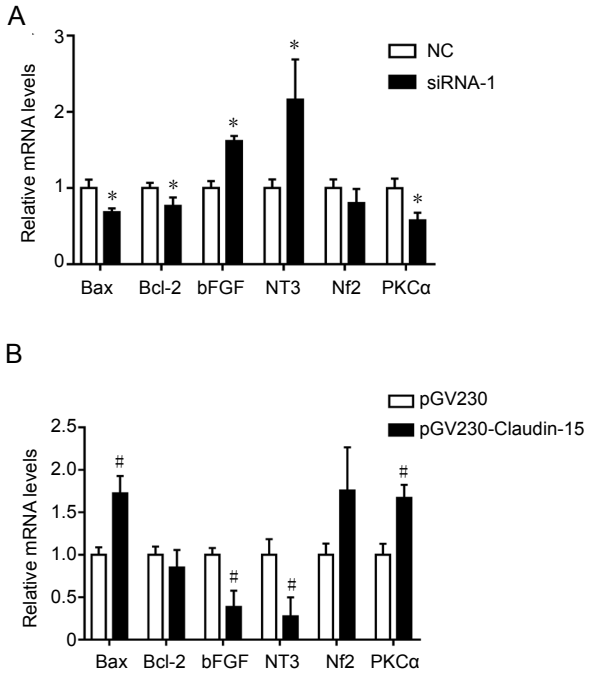

Figure 2 Gene expression changes in Claudin-15 siRNA-1 knockdown and pGV230-Claudin-15 overexpresed Schwann cells *in vitro*.

(A) Relative levels of Bax, Bcl-2, bFGF, NT3, Nf2 and PKCα mRNA expression of siRNA-1 transfected Schwann cells. GAPDH was used as normalizer. (B) Relative levels of Bax, Bcl-2, bFGF, NT3, Nf2 and PKCα mRNA expression of pGV230-Claudin-15 transfected Schwann cells. GAPDH was used as normalizer. $*P < 0.05$, *vs.* NC group; $\#P < 0.05$, *vs.* pGV230 group. All experiments were performed in triplicate. Data are shown as the mean ± SEM (unpaired Student's *t*-test). Bax: Bcl-2-associated X protein; Bcl-2: B-cell lymphoma 2; bFGF: basic fibroblast growth factor; GAPDH: glyceraldehyde-3-phosphate dehydrogenase; NC: negative control; Nf2: neurofibromin-2; NT3: neurotrophin-3; PKCα: protein kinase C alpha.

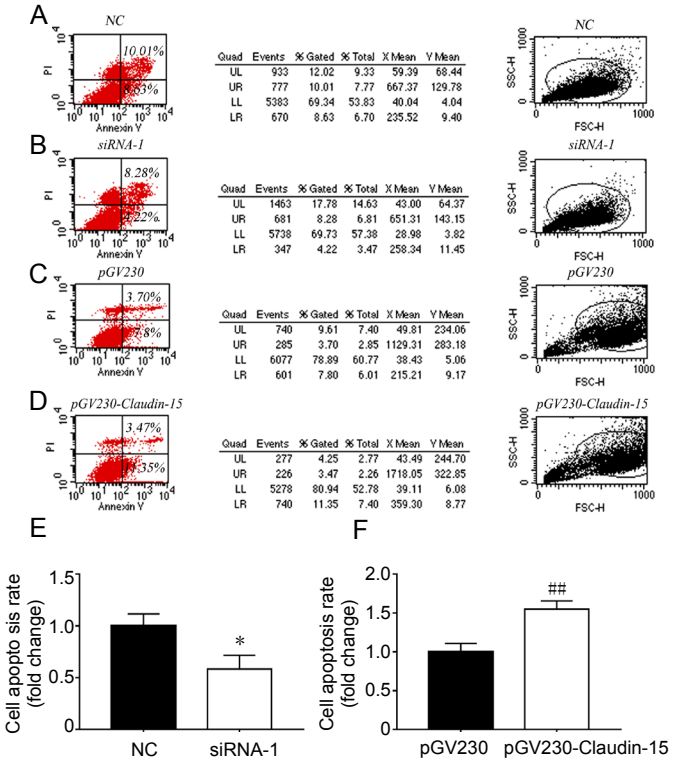

Figure 4 Claudin-15 knockdown and overexpression affect Schwann cells apoptosis (Annexin V-FITC/PI Assay) *in vitro*.

(A–D) Apoptosis of Schwann cells in the NC group (A), siRNA-1 group (B), pGV230 group (C) and p-GV230-Claudin-15 group (D) was measured by Annexin V-FITC/PI assay. (E) The rate of apoptosis of Schwann cells in the siRNA-1 group compared with NC group. (F) The rate of apoptosis of Schwann cells in pGV230-Claudin-15 group compared with pGV230 group. $*P < 0.05$, *vs.* NC group; $\#\#P < 0.01$, *vs.* pGV230 group. Average number of proliferating cells in NC or pGV230 group was set as 100%. The cell proliferation rate of p-GV230-Claudin-15 group was obtained by dividing its number of proliferating cells with the average number of proliferating cells in the NC or pGV230 group. The results were exhibited as fold change. All experiments were performed in triplicate. Data are shown as the mean ± SEM (unpaired Student's *t*-test). FITC: Fluorescein isothiocyanate; NC: negative control; PI: propidium iodide.

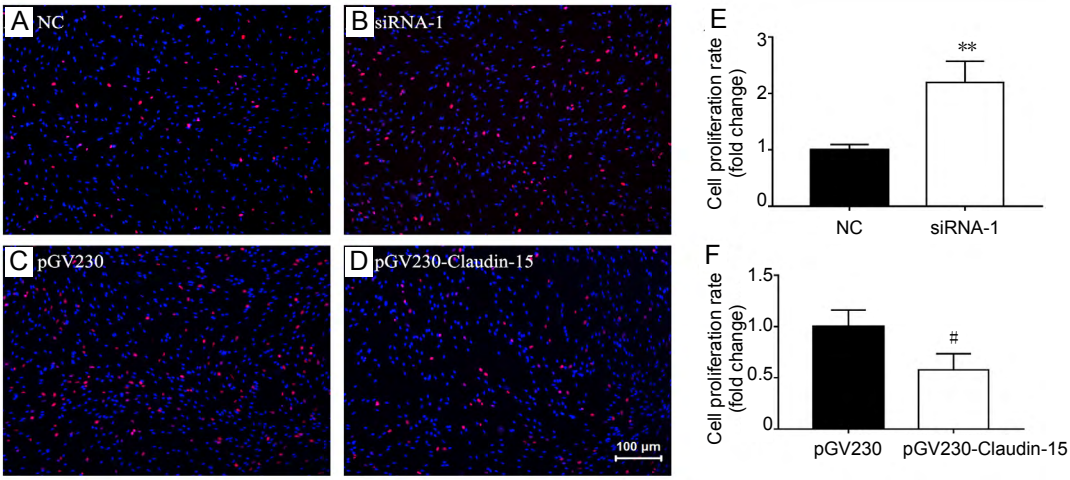

Figure 3 Claudin-15 knockdown and overexpression affect Schwann cells proliferation *in vitro*.

(A–D) Proliferation of Schwann cells in the NC (A), siRNA-1 (B), pGV230 (C), and pGV230-Claudin-15 (D) groups was determined by EdU staining. Images are taken by a fluorescence microscope. Merged image of EdU-positive Schwann cells (Red) and cell nuclei labeled by Hoechst 33342 (blue). Scale bar: 100 μm. (E) Cell proliferation rate of siRNA-1 group compared with NC group. (F) Cell proliferation rate of pGV230-Claudin-15 group compared with pGV230 group. $**P < 0.01$, *vs.* NC group; $\#P < 0.05$, *vs.* pGV230 group. All experiments were performed in triplicate. Data are shown as the mean ± SEM (unpaired Student's *t*-test). EdU: 5-Ethynyl-20-deoxyuridine; NC: negative control.

plasmid, their proliferation rate significantly decreased compared with the pGV230 group ($P < 0.05$; **Figure 3C**, **D,** and **F**). Schwann cells were stained with Hoechst 33342 (blue), and the proliferating cells were stained with Apollo 567 (red) (**Figure 3**). These results suggested that Claudin-15 expression inhibited Schwann cells proliferation *in vitro*.

Claudin-15 promotes Schwann cells apoptosis *in vitro*

To detect the apoptosis function of Claudin-15 on Schwann cells, siRNA-1, pGV230-Claudin-15 plasmid or negative control was used to transfect primary Schwann cells. The apoptotic rate of Schwann cells was lower in the siRNA-1 group than in the negative control group ($P < 0.05$; **Figure 4A**, **B,** and **E**). On the contrary, apoptotic rate was higher in the pGV230-Claudin-15 group than in the pGV230 group ($P < 0.05$; **Figure 4C**, **D,** and **F**). The results suggested that Claudin-15 promotes Schwann cells apoptosis.

Claudin-15 expression affects Schwann cells migration *in vitro*

To explore the effectiveness of Claudin-15 on Schwann cells *in vitro* further, we used the Transwell method to investigate the effects of Claudin-15 on Schwann cells migration. After transfection with siRNA, pGV230-Claudin-15 plasmid or negative control, the data showed that no significant changes were detected between the siRNA-1 and negative control groups (**Figure 5A**, **B,** and **E**); nor between the pGV230-Claudin-15 and pGV230 groups (**Figure 5C**, **D,** and **F**).

Silencing Claudin-15 downregulates c-Jun and AKT pathways *in vitro*

To identify the effect of Claudin-15 knockdown in Schwann cells, the signaling pathways and their phosphorylated (activated) ratios were investigated. The results showed that silencing Claudin-15 in cultured Schwann cells down-regulated c-Jun and AKT pathway expression (**Figure 6A**, **B**, and **D**). However, it had no effect on the ERK, β-catenin or c-Fos expression (**Figure 6C**, **E**, and **F**).

Claudin-15 overexpression upregulates c-Jun and c-Fos pathways *in vitro*

To identify the effect of Claudin-15 overexpression in Schwann cells, the signaling pathways and their phosphorylated (activated) ratios were investigated. The results showed that Claudin-15 overexpression up-regulated c-Jun and c-Fos expression in Schwann cells *in vitro* (**Figure 7A**, **D**, and **F**). However, there was no effect on AKT, ERK or β-catenin (**Figure 7B**, **C**, and **E**).

Discussion

In this study, we explored the effects of Claudin-15 on cell proliferation, apoptosis, migration ability and the signaling pathways of Schwann cells. The results suggested that Claudin-15 overexpression inhibited Schwann cell proliferation and promoted Schwann cell apoptosis, thereby activating PKCα, c-Jun, and Bax. Whereas silencing Claudin-15 reversed the above effects and provided neuroprotection for Schwann cells.

Schwann cells are the primary mediators of Wallerian degeneration after peripheral nerve injury. The proliferation, apoptosis and migration abilities of Schwann cells are crucial to Wallerian degeneration. Previously, we reported that Claudin-15 is up-regulated in Schwann cells during Wallerian degeneration (Li et al., 2013). Claudin-15 is mainly associated with the permeability and selectivity of cellular tight junctions (Tamura et al., 2011; Wada et al., 2013; Samanta et al., 2018). Other scientists found that Claudin-19 was not involved in the polarized morphogenesis of Schwann cells in peripheral myelinated axons (Miyamoto et al., 2005). We predicted Claudin-15 and Claudin-19 have similarities in their functions in Schwann cells.

Claudin-15 has been shown to play a role in cell migration (Takehara et al., 2009). β-Catenin, as part of the Wnt pathway, is also involved in cell migration (Yin et al., 2015). We used this to explore the effect of Claudin-15 on the migration of Schwann cells. However, our results did not show any association of Claudin-15 with the migration of Schwann cells. Moreover, there was no noticeable change in expression of β-catenin. Further experiments need to be carried out.

A few studies have shown that the Claudin family of proteins is associated with cell death and proliferation (Tsukita et al., 2008; Shimobaba et al., 2016). Our findings demonstrated that Claudin-15 induced Schwann cell apoptosis and inhibited their proliferating process. The quantitative polymerase chain reaction evidence showed that overexpression of Claudin-15 up-regulated PKCα and Bax and the activation ratio of p-c-Jun/c-Jun was up-regulated. PKCα is a serine threonine kinase upstream of the JNK pathway (Lampasso et al., 2002; Abou-Kandil et al, 2012; Jiang et al., 2017; Takami et al., 2018). Activating PKCα can induce apoptosis in many cell lines (Powell et al., 1996). The c-Jun and c-Fos participate in forming the transcription factor AP-1 downstream of the JNK pathway (Eferl and Wagner, 2003; Bi et al., 2018; Jin et al., 2018). Activation of c-Jun induced rapid cell death in cultured cells (Lei et al., 2002; Wang et al., 2017; Li et al., 2018). Bax is a key regulator of cell apoptosis (Campbell and Tait, 2018) and is essential for JNK-induced cell apoptosis (Lei et al., 2002; Weston and Davis, 2007). We predicted that Claudin-15 promotes Schwann cell apoptosis through the PKCα/JNK/Bax pathway.

AKT and ERK were key pro-survival factors inducing cell proliferation (Song et al., 2005; Huang et al., 2017). However, our study showed that the expression of activated AKT was down-regulated, whereas cell proliferation was upregulated by Claudin-15 knockdown. Furthermore, there was no statistical difference in ERK activation. Down-regulating PKCα may be responsible for the inactivation of AKT, since AKT can be activated by PKCα in conjunctival goblet cells (Li et al., 2013). We will continue to explore the pathways modifying cell proliferation of Schwann cells.

The main nerve regeneration regulators are bFGF, NT3 and Nf2 (Godinho et al., 2013; Truong et al., 2018; Wu et al., 2018). The up-regulation of bFGF and NT3 gene expression after Claudin15 knockdown showed that silencing Clau-

din-15 can be neuroprotective during Wallerian degeneration and/or nerve regeneration.

However, our results did not clarify how Claudin-15 affects Wallerian degeneration or nerve regeneration *in vivo*. Since Schwann cells have a decisive role in Wallerian degeneration and nerve regeneration, we predict that Claudin-15 may be a vital factor in Wallerian degeneration and nerve regeneration. Further studies of Claudin-15 functions *in vivo* may open new possibilities for providing insight into the mechanism of Claudins on nerve degeneration and/or regeneration.

Acknowledgments: *We greatly appreciate the editorial assistance of Te Zhang from China-Japan Union Hospital of Jilin University, China.*
Author contributions: *Experimental implementation: JNL; gene expression analysis: ZZ; data analysis: GZW; functional and biochemical data analysis: DBY, JNL; study planning: SSC; manuscript writing: JNL. All authors approved the final version of the paper.*
Conflicts of interest: *The authors declare that they have no competing interests.*
Financial support: *This study was supported by the National Natural Science Foundation of China, No. 81671220 (to SSC); the Scientific and Technological Development Program of Jilin Province of China, No. 20160101077JC (to SSC); the School Joint Construction Special Project of Jilin Province of China, No. SXGJQY2017-13 (to SSC). The funding sources had no role in study conception and design, data analysis or interpretation, paper writing or deciding to submit this paper for publication.*
Institutional review board statement: *All experimental procedures and protocols were approved by the Experimental Animal Ethics Committee of Jilin University of China (approval No. 2016-nsfc001) on March 5, 2016. The experimental procedure followed the United States National Institutes of Health Guide for the Care and Use of Laboratory Animals (NIH Publication No. 85-23, revised 1996).*
Copyright license agreement: *The Copyright License Agreement has been signed by all authors before publication.*
Data sharing statement: *Datasets analyzed during the current study are available from the corresponding author on reasonable request.*
Plagiarism check: *Checked twice by iThenticate.*
Peer review: *Externally peer reviewed.*

References

Abou-Kandil A, Chamias R, Huleihel M, Godbey WT, Aboud M (2012) Differential role of PKC-induced c-Jun in HTLV-1 LTR activation by 12-O-tetradecanoylphorbol-13-acetate in different human T-cell lines. PLoS One 7:e29934.

Alberini G, Benfenati F, Maragliano L (2018) Molecular dynamics simulations of ion selectivity in a claudin-15 paracellular channel. J Phys Chem B doi: 10.1021/acs.jpcb.8b06484.

Bi C, Cai Q, Shan Y, Yang F, Sun S, Wu X, Liu H (2018) Sevoflurane induces neurotoxicity in the developing rat hippocampus by upregulating connexin 43 via the JNK/c-Jun/AP-1 pathway. Biomed Pharmacother 108:1469-1476.

Cao P, Wang HN, Tian WF, Sun NC, Bai JB, Yu KL, Tian DH (2019) Human amniotic membrane repairs acute sciatic nerve injury in rat models. Zhongguo Zuzhi Gongcheng Yanjiu 23:1046-1051.

Campbell KJ, Tait SWG (2018) Targeting BCL-2 regulated apoptosis in cancer. Open Biol doi: 10.1098/rsob.180002.

Coleman MP, Freeman MR (2010) Wallerian degeneration, wld(s), and nmnat. Annu Rev Neurosci 33:245-267.

Conforti L, Gilley J, Coleman MP (2014) Wallerian degeneration: an emerging axon death pathway linking injury and disease. Nat Rev Neurosci 15:394-409.

Eferl R, Wagner EF (2003) AP-1: a double-edged sword in tumorigenesis. Nat Rev Cancer 3:859-868.

Garcia-Hernandez V, Quiros M, Nusrat A (2017) Intestinal epithelial claudins: expression and regulation in homeostasis and inflammation. Ann N Y Acad Sci 1397:66-79.

Geden MJ, Deshmukh M (2016) Axon degeneration: context defines distinct pathways. Curr Opin Neurobiol 39:108-115.

Gerdts J, Summers DW, Milbrandt J, DiAntonio A (2016) Axon self-destruction: new links among SARM1, MAPKs, and NAD+ metabolism. Neuron 89:449-460.

Girouard MP, Bueno M, Julian V, Drake S, Byrne AB, Fournier AE (2018) The molecular interplay between axon degeneration and regeneration. Dev Neurobiol 78:978-990.

Godinho MJ, Teh L, Pollett MA, Goodman D, Hodgetts SI, Sweetman I, Walters M, Verhaagen J, Plant GW, Harvey AR (2013) Immunohistochemical, ultrastructural and functional analysis of axonal regeneration through peripheral nerve grafts containing Schwann cells expressing BDNF, CNTF or NT3. PLoS One 8:e69987.

Gong L, Zhu Y, Xu X, Li H, Guo W, Zhao Q, Yao D (2014) The effects of claudin 14 during early Wallerian degeneration after sciatic nerve injury. Neural Regen Res 9:2151-2158.

Hagen SJ (2017) Non-canonical functions of claudin proteins: beyond the regulation of cell-cell adhesions. Tissue Barriers 5:e1327839.

Huang H, Liu H, Yan R, Hu M (2017) PI3K/Akt and ERK/MAPK signaling promote different aspects of neuron survival and axonal regrowth following rat facial nerve axotomy. Neurochem Res 42:3515-3524.

Jessen KR, Mirsky R (2016) The repair Schwann cell and its function in regenerating nerves. J Physiol 594:3521-3531.

Jessen KR, Arthur-Farraj P (2019) Repair schwann cell update: adaptive reprogramming, EMT, and stemness in regenerating nerves. Glia 67:421-437.

Jessen KR, Mirsky R (2019) The success and failure of the schwann cell response to nerve injury. Front Cell Neurosci 13:33.

Jiang R, Shi Y, Zeng C, Yu W, Zhang A, Du Y (2017) Protein kinase Calpha stimulates hypoxiainduced pulmonary artery smooth muscle cell proliferation in rats through activating the extracellular signal-regulated kinase 1/2 pathway. Mol Med Rep 16:6814-6820.

Jin X, Wang C, Wu W, Liu T, Ji B, Zhou F (2018) Cyanidin-3-glucoside alleviates 4-hydroxyhexenal-induced NLRP3 inflammasome activation via JNK-c-Jun/AP-1 pathway in human retinal pigment epithelial cells. J Immunol Res 2018:5604610.

Jortner BS (2019) Common structural lesions of the peripheral nervous system. Toxicol Pathol doi: 10.1177/0192623319826068.

Kennedy JM, Zochodne DW (2005) Impaired peripheral nerve regeneration in diabetes mellitus. J Peripher Nerv Syst 10:144-157.

Krause G, Protze J, Piontek J (2015) Assembly and function of claudins: structure-function relationships based on homology models and crystal structures. Semin Cell Dev Biol 42:3-12.

Krause G, Winkler L, Mueller SL, Haseloff RF, Piontek J, Blasig IE (2008) Structure and function of claudins. Biochim Biophys Acta 1778:631-645.

Lampasso JD, Marzec N, Margarone J, 3rd, Dziak R (2002) Role of protein kinase C alpha in primary human osteoblast proliferation. J Bone Miner Res 17:1968-1976.

Lei K, Fau NA, Zong WX, Kennedy NJ, Flavell RA, Thompson CB, Bar-Sagi D, Davis RJ, Davis RJ (2002) The Bax subfamily of Bcl2-related proteins is essential for apoptotic signal transduction by c-Jun NH(2)-terminal kinase. Mol Cell Biol 22:4929-4942.

Li D, Shatos MA, Hodges RR, Dartt DA (2013) Role of PKCalpha activation of Src, PI-3K/AKT, and ERK in EGF-stimulated proliferation of rat and human conjunctival goblet cells. Invest Ophthalmol Vis Sci 54:5661-5674.

Li J, Liu Y, Duan P, Yu R, Gu Z, Li L, Liu Z, Su L (2018) NFkappaB regulates HSF1 and cJun activation in heat stressinduced intestinal epithelial cell apoptosis. Mol Med Rep 17:3388-3396.

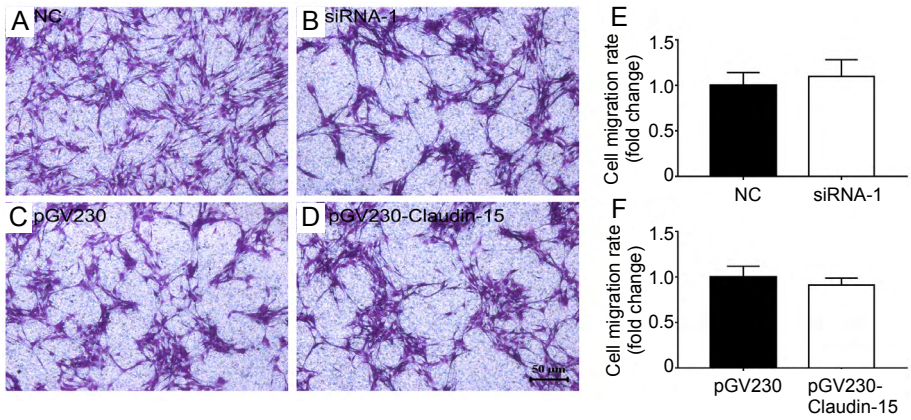

Figure 5 Claudin-15 knockdown and overexpression affect Schwann cells migration *in vitro*.
(A–D) Migrated Schwann cells in NC group (A), siRNA-1 group (B), pGV230 group (C) and pGV230-Claudin-15 group (D). Migrated Schwann cells were stained with crystal violet solution. Images are taken by an inverted light microscope. Scale bar: 50 μm. (E) Cell migration rate of Schwann cells in siRNA-1 group compared with NC group. (F) Cell migration rate of Schwann cells in pGV230-Claudin-15 group compared with pGV230 group. Assays were performed in triplicate. Data are shown as the mean ± SEM (unpaired Student's *t*-test). NC: Negative control.

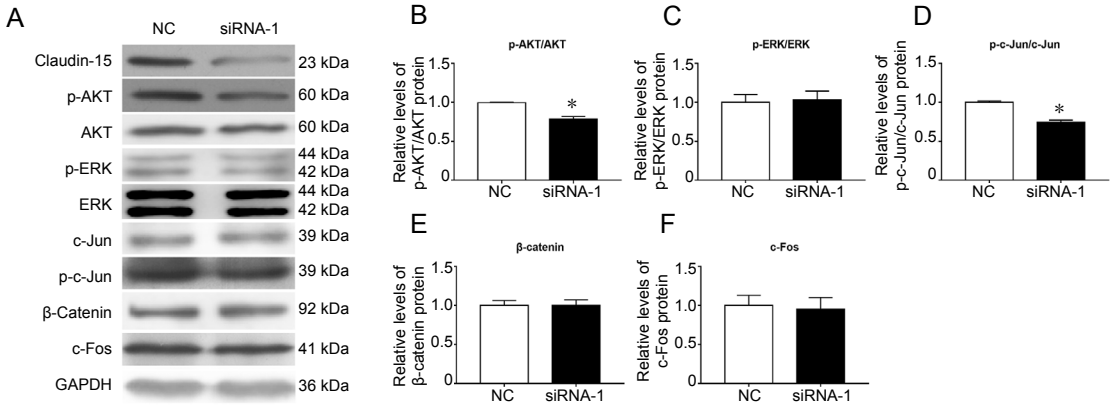

Figure 6 Silencing of Claudin-15 down-regulates AKT and c-Jun signaling pathways *in vitro*.
(A) Western blot assay of Claudin-15, p-AKT, AKT, p-ERK, ERK, c-Jun, p-c-Jun, β-catenin and c-Fos expression after siRNA-1 transfection. The top panels show target bands of Claudin-15, p-AKT, AKT, p-ERK, ERK, c-Jun, p-c-Jun, β-catenin and c-Fos. The bottom panel shows the loading control GAPDH. (B–D) Relative levels of p-AKT/AKT (B), p-ERK/ERK (C) and p-c-Jun/c-Jun (D) protein activation ratio after siRNA-1 transfected Schwann cells. (E, F) Relative levels of β-catenin (E) and c-Fos (F) protein expression of siRNA-1 transfected Schwann cells. $*P < 0.05$, *vs.* NC group. Average blot density of control group was set as 100%. The relative optical density value of p-GV230-Claudin-15 group was obtained by dividing its optical density with the optical density values of NC or pGV230 group. Assays were performed in triplicate. Data are shown as the mean ± SEM (unpaired Student's *t*-test). ERK: Extracellular signal-regulated kinase; GAPDH: glyceraldehyde-3-phosphate dehydrogenase; NC: negative control.

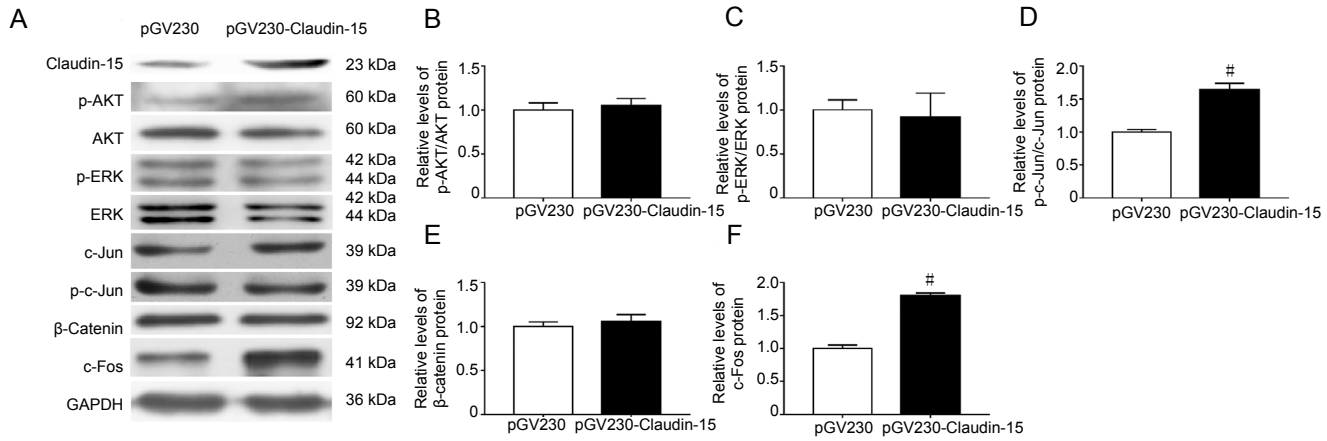

Figure 7 Overexpression of Claudin-15 activates c-Jun and c-Fos signaling pathways *in vitro*.
(A) Western blot assay of Claudin-15, p-AKT, AKT, p-ERK, ERK, c-Jun, p-c-Jun, β-catenin and c-Fos expression after pGV230-Claudin-15 transfection. The top panels show target bands of Claudin-15, p-AKT, AKT, p-ERK, ERK, c-Jun, p-c-Jun, β-catenin and c-Fos. The bottom panel shows the loading control GAPDH. (B–D) Relative levels of p-AKT/AKT (B), p-ERK/ERK (C) and p-c-Jun/c-Jun (D) protein activation ratio after pGV230-Claudin-15 transfected Schwann cells. (E, F) Relative levels of β-catenin (E) and c-Fos (F) protein expression of pGV230-Claudin-15 transfected Schwann cells. $\#P < 0.05$, *vs.* pGV230 group. Average blot density of control group blot was set as 100%. The relative optical density value of p-GV230-Claudin-15 group was obtained by dividing its optical density with the optical density values of NC or pGV230 group. Assays were performed in triplicate. Data are shown as the mean ± SEM (unpaired Student's *t*-test). ERK: Extracellular signal-regulated kinase; GAPDH: glyceraldehyde-3-phosphate dehydrogenase; NC: negative control.

Li M, Guo W, Zhang P, Li H, Gu X, Yao D (2013) Signal flow and pathways in response to early Wallerian degeneration after rat sciatic nerve injury. Neurosci Lett 536:56-63.

Li Y, Sun Y, Cai M, Zhang H, Gao N, Huang H, Cui S, Yao D (2018) Fas Ligand Gene (Faslg) plays an important role in nerve degeneration and regeneration after rat sciatic nerve injury. Front Mol Neurosci 11:210.

Lindborg JA, Mack M, Zigmond RE (2017) Neutrophils are critical for myelin removal in a peripheral nerve injury model of wallerian degeneration. J Neurosci 37:10258-10277.

Liou JT, Liu FC, Mao CC, Lai YS, Day YJ (2011) Inflammation confers dual effects on nociceptive processing in chronic neuropathic pain model. Anesthesiology 114:660-672.

Liu X, Yu X, He Y, Wang L (2019) Long noncoding RNA nuclear enriched abundant transcript 1 promotes the proliferation and migration of Schwann cells by regulating the miR-34a/Satb1 axis. J Cell Physiol doi: 10.1002/jcp.28302.

Mack TG, Reiner M, Beirowski B, Mi W, Emanuelli M, Wagner D, Thomson D, Gillingwater T, Court F, Conforti L, Fernando FS, Tarlton A, Andressen C, Addicks K, Magni G, Ribchester RR, Perry VH, Coleman MP (2001) Wallerian degeneration of injured axons and synapses is delayed by a Ube4b/Nmnat chimeric gene. Nat Neurosci 4:1199-1206.

Manole E, Ceafalan LC, Oproiu AM, Popa-Wagner A, Popescu BO (2015) Claudin-1 and occludin expression in demyelinating peripheral neuropathies. Rom J Morphol Embryol 56:1097-1102.

Miyamoto T, Morita K, Takemoto D, Takeuchi K, Kitano Y, Miyakawa T, Nakayama K, Okamura Y, Sasaki H, Miyachi Y, Furuse M, Tsukita S (2005) Tight junctions in Schwann cells of peripheral myelinated axons: a lesson from claudin-19-deficient mice. J Cell Biol 169:527-538.

Morita K, Furuse M, Fujimoto K, Tsukita S (1999) Claudin multigene family encoding four-transmembrane domain protein components of tight junction strands. Proc Natl Acad Sci U S A 96:511-516.

Muto S (2017) Physiological roles of claudins in kidney tubule paracellular transport. Am J Physiol Renal Physiol 312:F9-24.

Namikawa K, Okamoto T, Suzuki A, Konishi H, Kiyama H (2006) Pancreatitis-associated protein-III is a novel macrophage chemoattractant implicated in nerve regeneration. J Neurosci 26:7460-7467.

Powell CT, Brittis NJ, Stec D, Hug H, Heston WD, Fair WR (1996) Persistent membrane translocation of protein kinase C alpha during 12-0-tetradecanoylphorbol-13-acetate-induced apoptosis of LNCaP human prostate cancer cells. Cell Growth Differ 7:419-428.

Samanta P, Wang Y, Fuladi S, Zou J, Li Y, Shen L, Weber C, Khalili-Araghi F (2018) Molecular determination of claudin-15 organization and channel selectivity. J Gen Physiol 150:949-968.

Shefa U, Jung J (2019) Comparative study of microarray and experimental data on Schwann cells in peripheral nerve degeneration and regeneration: big data analysis. Neural Regen Res 14:1099-1104.

Shimobaba S, Taga S, Akizuki R, Hichino A, Endo S, Matsunaga T, Watanabe R, Yamaguchi M, Yamazaki Y, Sugatani J, Ikari A (2016) Claudin-18 inhibits cell proliferation and motility mediated by inhibition of phosphorylation of PDK1 and Akt in human lung adenocarcinoma A549 cells. Biochim Biophys Acta 1863:1170-1178.

Siemionow M, Brzezicki G (2009) Chapter 8: Current techniques and concepts in peripheral nerve repair. Int Rev Neurobiol 87:141-172.

Simon DJ, Pitts J, Hertz NT, Yang J, Yamagishi Y, Olsen O, Tesic Mark M, Molina H, Tessier-Lavigne M (2016) Axon degeneration gated by retrograde activation of somatic pro-apoptotic signaling. Cell 164:1031-1045.

Song G, Ouyang G, Bao S (2005) The activation of Akt/PKB signaling pathway and cell survival. J Cell Mol Med 9:59-71.

Stoll G, Jander S, Myers RR (2002) Degeneration and regeneration of the peripheral nervous system: from Augustus Waller's observations to neuroinflammation. J Peripher Nerv Syst 7:13-27.

Takami M, Katayama K, Noguchi K, Sugimoto Y (2018) Protein kinase C alpha-mediated phosphorylation of PIM-1L promotes the survival and proliferation of acute myeloid leukemia cells. Biochem Biophys Res Commun 503:1364-1371.

Takehara M, Nishimura T, Mima S, Hoshino T, Mizushima T (2009) Effect of claudin expression on paracellular permeability, migration and invasion of colonic cancer cells. Biol Pharm Bull 32:825-831.

Tamura A, Hayashi H, Imasato M, Yamazaki Y, Hagiwara A, Wada M, Noda T, Watanabe M, Suzuki Y, Tsukita S (2011) Loss of claudin-15, but not claudin-2, causes Na+ deficiency and glucose malabsorption in mouse small intestine. Gastroenterology 140:913-923.

Tetzlaff W (1982) Tight junction contact events and temporary gap junctions in the sciatic nerve fibres of the chicken during Wallerian degeneration and subsequent regeneration. J Neurocytol 11:839-858.

Truong K, Ahmad I, Jason Clark J, Seline A, Bertroche T, Mostaert B, Van Daele DJ, Hansen MR (2018) Nf2 mutation in schwann cells delays functional neural recovery following injury. Neuroscience 374:205-213.

Tsukita S, Tanaka H, Tamura A (2019) The claudins: from tight junctions to biological systems. Trends Biochem Sci 44:141-152.

Tsukita S, Yamazaki Y, Katsuno T, Tamura A, Tsukita S (2008) Tight junction-based epithelial microenvironment and cell proliferation. Oncogene 27:6930-6938.

Van Itallie CM, Anderson JM (2006) Claudins and epithelial paracellular transport. Annu Rev Physiol 68:403-429.

Wada M, Tamura A, Takahashi N, Tsukita S (2013) Loss of claudins 2 and 15 from mice causes defects in paracellular Na^+ flow and nutrient transport in gut and leads to death from malnutrition. Gastroenterology 144:369-380.

Waller A (1851) Experiments on the section of the glosso-pharyngeal and hypoglossal nerves of the frog, and observations of the alterations produced thereby in the structure of their primitive fibres. Edinb Med Surg J 76:369-374.

Wang K, Jin S, Fan D, Wang M, Xing N, Niu Y (2017) Anti-proliferative activities of finasteride in benign prostate epithelial cells require stromal fibroblasts and c-Jun gene. PLoS One 12:e0172233.

Wang Y, Song M, Song F (2018) Neuronal autophagy and axon degeneration. Cell Mol Life Sci 75:2389-2406.

Weston CR, Davis RJ (2007) The JNK signal transduction pathway. Curr Opin Cell Biol 19:142-149.

Williams PA, Harder JM, Foxworth NE, Cardozo BH, Cochran KE, John SWM (2017) Nicotinamide and WLD(S) act together to prevent neurodegeneration in glaucoma. Front Neurosci 11:232.

Wu Y, Wang Z, Cai P, Jiang T, Li Y, Yuan Y, Li R, Khor S, Lu Y, Wang J, Chen D, Zeng Q, Zhong R, Zhang H, Lin Y, Li X, Xiao J (2018) Dual delivery of bFGF- and NGF-binding coacervate confers neuroprotection by promoting neuronal proliferation. Cell Physiol Biochem 47:948-956.

Yi S, Liu Q, Wang X, Qian T, Wang H, Zha G, Yu J, Wang P, Gu X, Chu D, Li S (2019) Tau modulated Schwann cell proliferation, migration, and differentiation following peripheral nerve injury. J Cell Sci doi:10.1242/jcs.222059.

Yin J, Zeng F, Wu N, Kang K, Yang Z, Yang H (2015) Interleukin-8 promotes human ovarian cancer cell migration by epithelial-mesenchymal transition induction in vitro. Clin Transl Oncol 17:365-370.

Zhang H, Shao Z, Zhu Y, Shi L, Li Z, Hou R, Zhang C, Yao D (2018) Toll-like receptor 4 (TLR4) expression affects schwann cell behavior in vitro. Sci Rep 8:11179.

Zigmond RE, Echevarria FD (2019) Macrophage biology in the peripheral nervous system after injury. Prog Neurobiol 173:102-121.

C-Editor: Zhao M; S-Editors: Wang J, Li CH; L-Editors: Dawes EA, Haase R, Qiu Y, Song LP; T-Editor: Jia Y